Journal of Solid State Chemistry 181 (2008) 2020–2023

Contents lists available at ScienceDirect

Journal of Solid State Chemistry

journal homepage: www.elsevier.com/locate/jssc

# Fabrication and optical conductivities of strained epitaxial $Na_xCoO_2$ thin films: $x = 0.5$, 0.7

J.Y. Son, Y.H. Shin, C.S. Park *

*Department of Materials Science and Engineering, Pohang University of Science and Technology (POSTECH), Pohang 790-784, Republic of Korea*

ARTICLE INFO

*Article history:*
Received 3 March 2008
Received in revised form
1 May 2008
Accepted 3 May 2008
Available online 10 May 2008

*Keywords:*
Epitaxial thin films
$Na_{0.5}CoO_2$
$Na_{0.7}CoO_2$
Optical conductivity
Na deintercalation

ABSTRACT

Epitaxial $\gamma$ phase-$Na_xCoO_2$ thin films were deposited on (001) sapphire by the pulsed laser deposition method. To fabricate epitaxial $Na_{0.5}CoO_2$ thin films, we used a solution of iodine-dissolved acetonitrile and obtained an epitaxial $Na_{0.5}CoO_2$ thin film with a high crystallinity because of Na deintercalation of epitaxial $Na_{0.7}CoO_2$. From the spectroscopic ellipsometry analysis, we obtained the optical constants as well as the optical conductivities for the $Na_{0.5}CoO_2$ and $Na_{0.7}CoO_2$ thin films. The energy splitting between $e_g$ and $a_{1g}$ increased because of the structural strain of the $Na_{0.7}CoO_2$ thin film. It is inferred that the structural strain is the source for the lower resistivity and the preservation of the strongly correlated system up to 200 K for the $Na_{0.7}CoO_2$ thin film. On the other hand, the strain in the $Na_{0.5}CoO_2$ thin film was not affected, and the charge-ordering state and the Na content ($x = 0.5$) only cause the charge-ordering state.



## 1. Introduction

Sodium cobalt oxide $Na_xCoO_2$ is a good thermoelectric material that shows a large thermoelectric power and a low resistivity, and its large thermoelectric power is attributed to the spin entropy from the low spin state of the Co ion [1,2]. Especially, under the variation of the sodium content $x$, $Na_xCoO_2$ exhibits complicate transport behaviors as a strongly correlated electron system with various magnetic orderings. The metallic state remained as a paramagnetic metal at the range of $0<x<0.5$, "Curie–Weiss" metal (anitiferromagnetic ordering) at the range of $0.5<x<0.7$, spin-density wave (SDW) metal at the range of $0.7<x<1$, while the insulating state as a charge-ordering state of anitiferromagnetic ordering at $x = 1/2$ and a band insulator at $x = 1$ [3–5]. Moreover, the discovery of superconductivity in $Na_{0.35}CoO_2 \cdot 1.3H_2O$ with $T_C$ about 5 K made sodium cobalt oxide $Na_xCoO_2$ an interesting subject [6].

Behind the rich phase diagrams and interesting physical properties, there are strongly correlated 3$d$ electrons of Co ion at the two-dimensional transition-metal oxide triangular lattice, which can bring into geometrical frustration of the Co spins [4]. A fraction of $Co^{3+}$ and $Co^{4+}$ is decided by a sodium content $x$ because sodium ions act as a donor and they make a $Co^{3+}$ of spin $S = 0$ from a $Co^{4+}$ of spin $S = 1/2$; hence, a current flow is generated by the hopping of a hole (spin $S = -1/2$) at $Co^{4+}$ ions to $Co^{3+}$ ions in a diamagnetic background [2]. In $\gamma$-$Na_xCoO_2$, the in-plane direction of $CoO_6$ octahedron in the $CoO_2$ layer alternates with the nearest $CoO_2$ layers, and $CoO_6$ octahedron is a trigonal distorted, which split $t_{2g}$ states into $a_{1g}$ ($3z^2-r^2$) and $e'_g$ states [7]. Therefore, to understand the orbital character of the valence electrons is an important issue, which was intensively researched by experimental and theoretical approaches such as X-ray absorption spectra (XAS) experiments and band structure calculations in the local density approximation (LDA) [8,9].

To understand the electron states of $Na_xCoO_2$, we depicted the trigonal distortion of $CoO_6$ with $D_{3d}$ symmetry and $e_g$, $a_{1g}$ ($3z^2-r^2$) and $e'_g$ states (Fig. 1). Based on the LDA calculations of the $Na_xCoO_2$, the O 2$p$ bands with the band width of 5 eV exist under the Fermi energy at a distance of 2 eV and the hybridization of Co 3$d$ and O 2$p$ is weak [9]. For the comprehension about the optical properties in $Na_xCoO_2$, Figs. 2(a)–(c) delineate suitable transitions from an initial state to a final state in the $a_{1g}$ ($3z^2-r^2$) and $e'_g$ states. The initial state in Figs. 2(a) and (b) indicate the $a_{1g}$ ($3z^2-r^2$) and the $e'_g$ states in the $Co^{4+}$ of spin $S = 1/2$ and the initial state in Fig. 2(c) represents the $a_{1g}$ ($3z^2-r^2$) and the $e'_g$ states in the $Co^{3+}$ of spin $S = 0$. Therefore, the transition probabilities (A and B transitions) in Figs. 2(a) and (b) decrease with increasing the sodium content in $Na_xCoO_2$. On the other hand, an increase of the sodium content in $Na_xCoO_2$ raises the transition probability (C transitions) in Fig. 2(c).

In this study, we analyzed the spectroscopic ellipsometry data to study the optical properties of epitaxial layered cobaltite $Na_xCoO_2$ thin films for $x = 0.7$ and 0.5. In the previous report, the structure of the $Na_xCoO_2$ thin film was controlled from a $\beta$-phase

* Corresponding author. Fax: +82 54 279 2399.
*E-mail address:* cslpark@postech.ac.kr (C.S. Park).

0022-4596/$ - see front matter Crown Copyright © 2008 Published by Elsevier Inc. All rights reserved.
doi:10.1016/j.jssc.2008.05.005

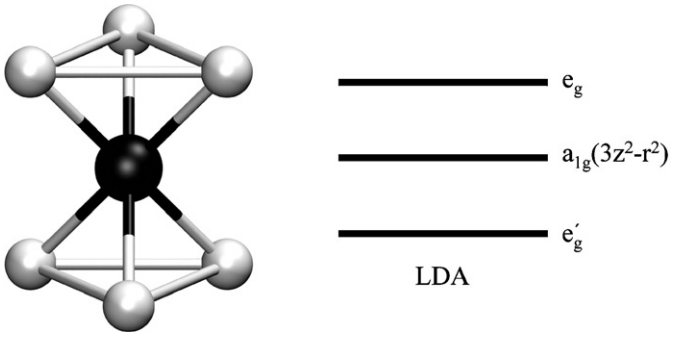


**Fig. 1.** The trigonal distortion of the $CoO_6$ with $D_{3d}$ symmetry (left). Crystal field splitting of Co 3*d* states in the distorted $CoO_6$ (right).

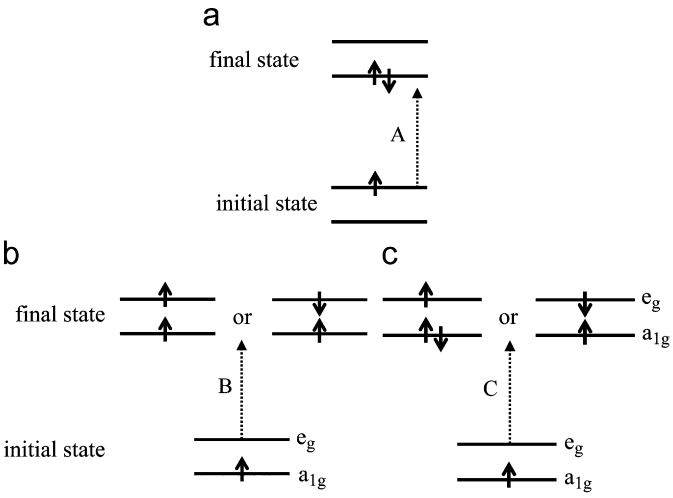


**Fig. 2.** (a–c) Transitions from the initial state to the final state in the low-spin state.

with an island growth mode to a $\gamma$-phase with a layer-by-layer growth mode by the reduction of the deposition rate [10]. Here, we fabricated the epitaxial $\gamma$-$Na_{0.5}CoO_2$ thin film, which is well known as the Mott insulator, by the sodium deintercalation of the epitaxial $\gamma$-$Na_{0.7}CoO_2$ thin film in a solution of iodine-dissolved acetonitrile. We obtained the optical constants and the optical conductivities of the $Na_{0.5}CoO_2$ and $Na_{0.7}CoO_2$ thin films by ellipsometer analysis.

## 2. Experiment

$Na_{0.7}CoO_2$ thin films were deposited on a (001) sapphire by the PLD method and the lattice misfit between *c*-oriented $\gamma$-$Na_{0.7}CoO_2$ and the (001) sapphire is 2.9% compressive. The $Na_{0.8}CoO_2$ target, which was used in PLD, was prepared by a conventional solid-state reaction method [9]. A frequency-tripled (355 nm, ~2 J/cm$^2$) Nd:YAG laser was used for deposition, and the distance between the target and the substrate was ~4 cm. The substrate temperature of optimal thin film growth was 480 °C and the optimal oxygen pressure of 400 mTorr was maintained during deposition. The deposition rate and the energies of adatoms were simultaneously reduced by an eclipse method because direct high-energy particles would be rejected by a shadow mask. The $\gamma$-$Na_{0.7}CoO_2$ thin film was grown with a layer-by-layer growth mode by the low deposition rate of 0.02 Å/pulse using the eclipse method on (001) sapphire substrates. For the structural determinations of $\beta$- and $\gamma$-$Na_xCoO_2$ thin films, X-ray diffraction data were obtained by a high-resolution X-ray diffractometer (Cu*K* radiation, 1.542 Å), in which $2\theta$ values had data with the interval of 0.01°. From this $2\theta$ value, we calculated lattice constants with the error below 0.002 Å. The thicknesses of $Na_xCoO_2$ thin films were ~200 nm, determined from the cross-sectional images of scanning electron microscope (SEM). The surface morphologies and topographies of $Na_{0.5}CoO_2$ and $Na_{0.7}CoO_2$ thin films were observed by SEM and atomic force microscope (AFM).

To deintercalate the sodium in the $Na_{0.7}CoO_2$ thin film, we used the dissolved $I_2$ (0.05 molar, 99.999%) solution in acetonitrile (99.99%), and after the sodium deintercalation, samples were washed in pure acetonitrile (99.99%) and dried by $N_2$ gas (99.99%). After the dipping of $Na_{0.7}CoO_2$ thin films in $I_2$ solution at room temperature, samples were fabricated for 2 days at intervals of 6 h. Based on this experiment, we could control a more precise composition near 2 days under intervals of 30 min. From this precise control of the deintercalation time, the $Na_{0.5}CoO_2$ composition with error below 5% was elaborately achieved and this composition was confirmed by an energy-dispersive X-ray spectrometer (EDS) and the charge-ordered behavior of resistivity data.

## 3. Results and discussion

To check the variation of the lattice constant along the out-of-plane, we carried out $\theta$–$2\theta$ scans of the $Na_{0.5}CoO_2$ and $Na_{0.7}CoO_2$ thin films. Fig. 3 shows the (002) XRD peaks of $Na_{0.5}CoO_2$ and $Na_{0.7}CoO_2$ thin films grown on a (001) sapphire substrate. The shift of the (002) peak is observed, indicating the increase of the lattice constant along the out-of-plane, and this variation of the lattice constant results from sodium deintercalation. From the positions of two (002) XRD peaks, lattice constants of 11.32 and 10.85 Å were calculated, which are slightly different values from the bulk lattice constants of single crystals (11.11 Å for $x = 0.5$, 10.97 Å for $x = 0.7$) [3]. The full width at half maximums (FWHMs) of two (002) XRD peaks are 0.5 and 0.4° for $x = 0.5$ and 0.7, respectively. From this variation of the FWHMs, it is inferred that the $Na_{0.5}CoO_2$ thin film has a more strained structure than the $Na_{0.7}CoO_2$ thin film as a result of sodium deintercalation.

To acquire microstructure information along the in-plane, we performed X-ray scattering with $\Phi$-scan geometry (not shown). The sixfold symmetries of two (104) peaks were observed, which represent the hexagonal structures of $Na_{0.5}CoO_2$ and $Na_{0.7}CoO_2$ thin films with twinning. The FWHMs of two (104) peaks are equal to 0.5° and 0.35° for the $Na_{0.5}CoO_2$ and $Na_{0.7}CoO_2$ thin films, respectively. From this increase of the FWHM, it is inferred that the crystallinity of $Na_{0.5}CoO_2$ along the in-plane is also influenced by sodium deintercalation. From the $2\theta$ values of two (104) peaks, we obtained the hexagonal *a*-axis lattice constants of 2.81 and 2.82 Å for $Na_{0.5}CoO_2$ and $Na_{0.7}CoO_2$ thin films, and these values are slightly reduced from the *a*-lattice constant of the single-crystal $Na_{0.7}CoO_2$. It is inferred that this small change of the *a*-lattice constant is due to the relative high change of the *c*-lattice constant and also confirm the high Young's modulus of $CoO_2$ layers. Based on the XRD data along the out-of-plane and in-plane, we found that sodium deintercalation only elongated a *c*-lattice constant of $Na_xCoO_2$.

We checked resistivities as a function of temperature for $Na_{0.5}CoO_2$ and $Na_{0.7}CoO_2$ thin films as shown in Fig. 4. The $Na_{0.5}CoO_2$ thin film exhibits an insulating transport behavior with three weak anomalies as a charge-ordered insulator below 100 K, which is similar to the $Na_{0.5}CoO_2$ single crystal [3]. For the $Na_{0.5}CoO_2$ single crystal, there were two anomalies in the resistivity data as a function of temperature although the magnetic susceptibility data as a function of temperature had

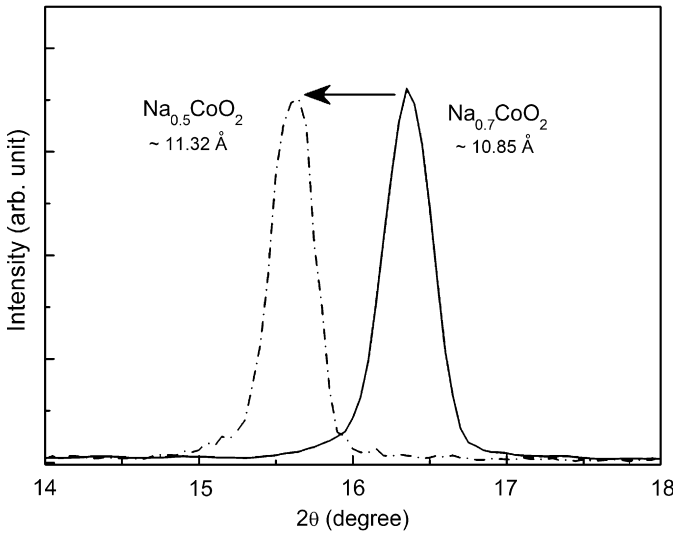


**Fig. 3.** (002) XRD peaks of $Na_{0.5}CoO_2$ and $Na_{0.7}CoO_2$ thin films. This shift of the (002) peak means an increase of the *c*-lattice constant resulting from the Na deintercalation.

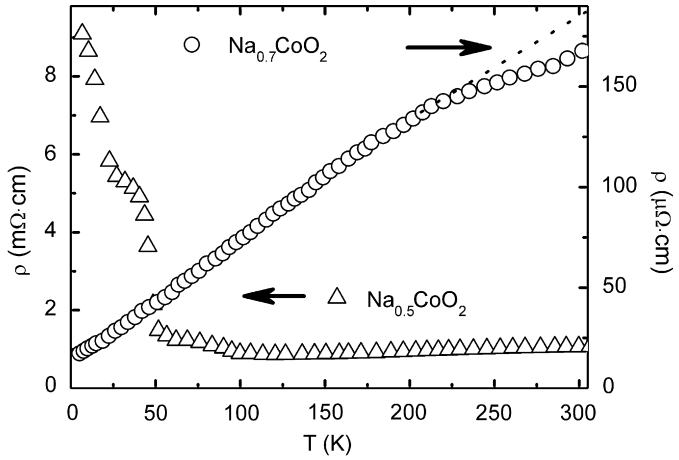


**Fig. 4.** Resistivities of $Na_{0.5}CoO_2$ and $Na_{0.7}CoO_2$ thin films. The resistivity of $Na_{0.7}CoO_2$ thin film shows a metallic property similar to the resistivity of $Na_{0.7}CoO_2$ single crystal. The $Na_{0.5}CoO_2$ exhibits the transport behavior of a charge-ordered insulator.

three anomalies. Thus, we inferred that the anomaly near 90 K is clearly observed by the enhanced crystallinity of the $Na_{0.5}CoO_2$ thin film. The resistivity of the $Na_{0.7}CoO_2$ thin film shows a metallic property similar to the resistivity of the $Na_{0.7}CoO_2$ single crystal. At 300, the resistivity of the $Na_{0.7}CoO_2$ thin film is about 177 μΩ cm, which is lower than the $Na_{0.7}CoO_2$ single crystal. In $Na_xCoO_2$, the Co ion has a two-dimensional triangular lattice and a low spin state of $Co^{3+}$ or $Co^{4+}$, and the oxygen 2*p* states are lower than the cobalt 3*d* states. A fraction of $Co^{3+}$ and $Co^{4+}$ is decided by a sodium content *x* because sodium ions act as a donor and they make a $Co^{3+}$ of spin $S=0$ from a $Co^{4+}$ of spin $S=1/2$. A current flow is caused by the hopping of a hole (spin $S=-1/2$) at $Co^{4+}$ ions to $Co^{3+}$ ions in a diamagnetic background. Up to 200 K, the temperature dependence of the resistivity of the $Na_{0.7}CoO_2$ thin film shows a linear variation, indicating the transport behavior of a strongly correlated system. This linear resistivity means the "Curie–Wiess" metallic behavior of the $Na_{0.7}CoO_2$ thin film [2].

For the optical property, we analyzed the spectroscopic ellipsometry data of the epitaxial layered cobaltite $Na_{0.5}CoO_2$ and $Na_{0.7}CoO_2$ thin films with and the incident angle of 70° by a multiwavelength variable-angle ellipsometer (J. A. Woollam Co.). At the energy range of 0.7–6.0 eV, ellipsometry parameters of $\Psi$ and $\Delta$ were measured and these parameters are defined by $R_\rho/R_S = \tan\Psi\exp(i\Delta)$, where $R_\rho$ and $R_S$ are complex reflection coefficients for polarized light parallel and perpendicular to the plane of incidence, respectively. Based on the Levenberg–Marquardt algorithm, we fit $\Psi'$ and $\Delta'$ for the model of $Na_xCoO_2$ thin films on $Al_2O_3$ substrate to the experimental parameter $\Psi$ and $\Delta$ at the incident angle of 70° and the energy range of 0.7–6.0 eV [11].

From the data fitting, we obtained the refractive index *n* and the extinction coefficient *k* of $Na_xCoO_2$ thin films and the complex refractive index is expressed by $\hat{n} = n + ik$. The complex dielectric function and the optical absorption coefficient are directly obtained by $\varepsilon_1 = n^2 - k^2$, $\varepsilon_2 = 2nk$ and $\alpha = 4\pi k/\lambda$, where $\lambda$ is the wavelength of incident photons. Figs. 5(a) and (b) show the refractive indices *n* and the extinction coefficients *k* of $Na_{0.5}CoO_2$ and $Na_{0.7}CoO_2$ thin films. The $Na_{0.5}CoO_2$ and $Na_{0.7}CoO_2$ thin films show high refractive indices and the refractive index decreases with increasing photon energy. The extinction coefficients increase with increasing photon energy and this decrease of the refractive indices is because photon speed in the films is influenced by optical absorption. In addition, there are two or three peaks in the extinction coefficients, which result from intraband transitions in 3*d* of Co ions.

Optical conductivities of $Na_{0.5}CoO_2$ and $Na_{0.7}CoO_2$ thin films were calculated from the refractive index *n* and the extinction coefficient *k* (Fig. 6). Three peaks are observed, which correspond

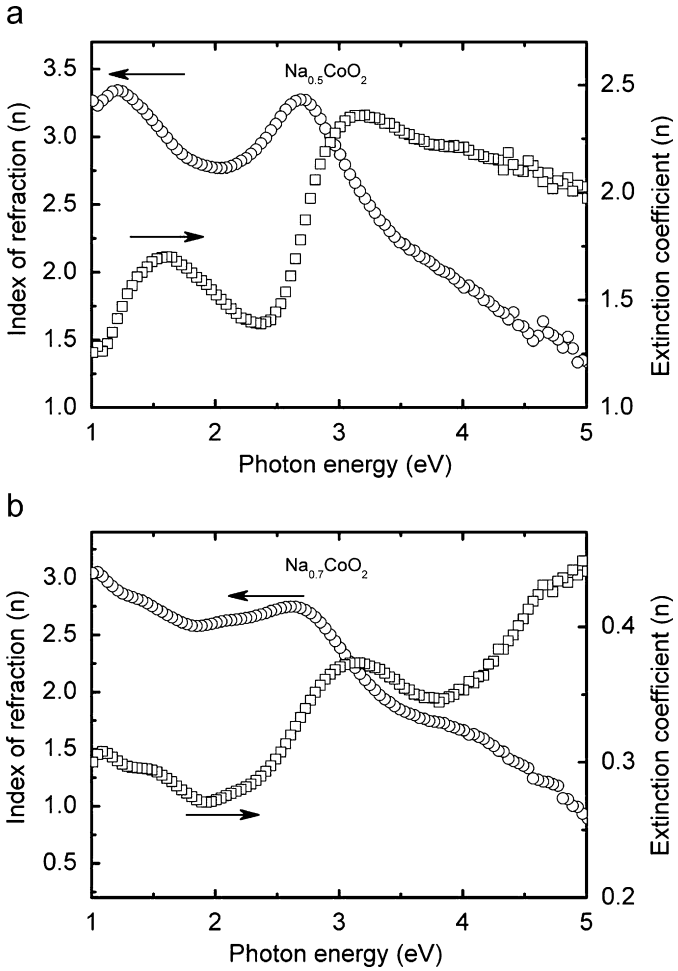


**Fig. 5.** Refractive index *n* and extinction coefficient *k*. (a) $Na_{0.5}CoO_2$ thin film and (b) $Na_{0.7}CoO_2$ thin film.

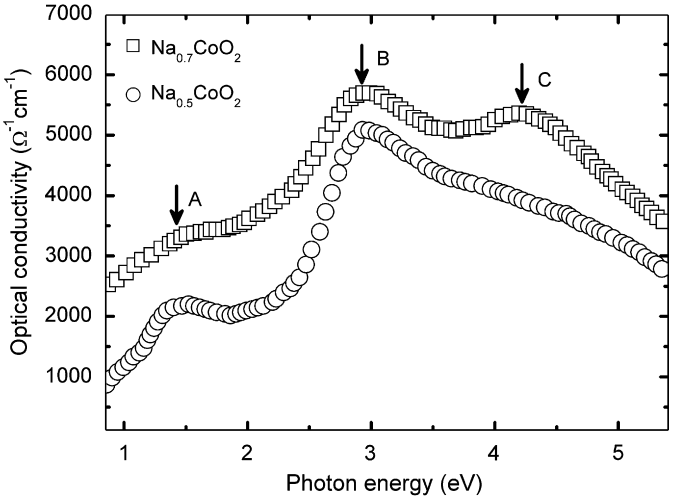


**Fig. 6.** Optical conductivities of $Na_{0.5}CoO_2$ and $Na_{0.7}CoO_2$ thin films.

to A, B and C transitions of the $Na_{0.7}CoO_2$ thin film in Fig. 2. For the $Na_{0.5}CoO_2$ thin film, the C transition is very weak, indicating that the population of $Co^{4+}$ in the $Na_{0.5}CoO_2$ thin film is smaller than that in the $Na_{0.7}CoO_2$ thin film. The optical conductivities of the $Na_{0.5}CoO_2$ and $Na_{0.7}CoO_2$ thin films properly reflected the transitions of 3*d* electrons in a low spin state of Co ions [9,12]. For the $Na_{0.7}CoO_2$ thin film, the difference of photon energies between the A and B transitions and the difference of photon energies between the B and C transitions are about 1.8 and 1.6 eV, respectively. These differences are larger than that of a $Na_{0.7}CoO_2$ single crystal (1.02 eV between the B and C transitions and 0.88 eV between the B and C transitions), which are well reflected in the strained structure of the $Na_{0.7}CoO_2$ thin film. This also means that the energy splitting between $e_g$ and $a_{1g}$ increased as a result of the strained structure in the $Na_{0.7}CoO_2$ thin film that causes a distortion of the $CoO_6$ octahedron. Thus, it is suggested that this increase of energy splitting can be the source of the lower resistivity and the preservation of the strongly correlated system up to 200 K for the $Na_{0.7}CoO_2$ thin film.

## 4. Conclusion

We analyzed the spectroscopic ellipsometry data to study the optical properties of epitaxial layered cobaltite $Na_xCoO_2$ thin films for $x = 0.7$ and 0.5. We obtained the optical constants as well as the optical conductivities of the $Na_{0.5}CoO_2$ and $Na_{0.7}CoO_2$ thin films from on the ellipsometer analysis. The optical conductivities of the $Na_{0.5}CoO_2$ and $Na_{0.7}CoO_2$ thin films properly reflect the transitions of 3*d* electrons in a low spin state of Co ions. The energy splitting between $e_g$ and $a_{1g}$ increased as a result of the distortion of the octahedron in the $Na_{0.7}CoO_2$ thin film, which can be the source of the lower resistivity and the preservation of the strongly correlated system up to 200 K for the $Na_{0.7}CoO_2$ thin film. In the $Na_{0.7}CoO_2$ thin film, the strain induces the low resistivity. On the other hand, the strain in the $Na_{0.5}CoO_2$ thin film did not affect the charge-ordering state and the Na content ($x = 0.5$) only causes the charge-ordering state.

## Acknowledgments

This work was supported by Brain Korea 21 Project 2008.

## References

[1] I. Terasaki, Y. Sasago, K. Uchinokura, Phys. Rev. B 56 (1997) R12685–R12687.
[2] Y. Wang, Nyriss S. Rogado, R.J. Cava, N.P. Ong, Nature 423 (2003) 425–428.
[3] M.L. Foo, Y.Y. Wang, S. Watauchi, H.W. Zandbergen, T. He, R.J. Cava, N.P. Ong, Phys. Rev. Lett. 92 (2004) 247001–247004.
[4] M. Roger, D.J.P. Morris, D.A. Tennant, M.J. Gutmann, J.P. Goff, J.-U. Hoffmann, R. Feyerherm, E. Dudzik, D. Prabhakaran, A.T. Boothroyd, N. Shannon, B. Lake, P.P. Deen, Nature 445 (2007) 631–634.
[5] H.W. Zandbergen, M. Foo, Q. Xu, V. Kumar, R.J. Cava, Phys. Rev. B 70 (2004) 024101–024108.
[6] Kazunori Takada, Hiroya Sakurai, Eiji Takayama-Muromachi, Fujio Izumi1, Ruben A. Dilanian, Takayoshi Sasaki, Nature 422 (2003) 53–55.
[7] G. Baskaran, Phys. Rev. Lett. 91 (2003) 097003–097006.
[8] T. Kroll, A.A. Aligia, G.A. Sawatzky, Phys. Rev. B. 74 (2006) 115124.
[9] D.J. Singh, Phys. Rev. B. 61 (2000) 13397–13402.
[10] J.Y. Son, Bog G. Kim, J.H. Cho, Appl. Phys. Lett. 86 (2005) 221918–221921.
[11] A. Canillas, E. Pascual, B. Drevillon, Rev. Sci. Instrum. 64 (1993) 2153–2159.
[12] W.B. Wu, D.J. Huang, J. Okamoto, A. Tanaka, H.J. Lin, F.C. Chou, A. Fujimori, C.T. Chen, Phys. Rev. Lett. 94 (2005) 146402–146405.